

Field enhancement and harmonic generation in ϵ -near-zero substrates under oblique TM-polarized illumination

S. Campione¹, M. A. Vincenti², D. de Ceglia², M. Scalora³, F. Capolino¹

¹Department of Electrical Engineering and Computer Science

University of California Irvine

4131 Engineering Hall, CA-92697, Irvine, USA

Fax: +1-949-824-1853; email: scampion@uci.edu; f.capolino@uci.edu

²Aegis Technologies Inc

410 Jan Davis Dr, AL-35806, Huntsville, USA

Fax: +1-256-842-2507; email: mvincenti@aegistg.com; ddeceglia@aegistg.com

³US Army Charles M. Bowden Research Center, RDECOM

Redstone Arsenal, AL-35898, Huntsville, USA

Fax: +1-256-842-2507; email: michael.scalora@us.army.mil

Abstract

We investigate local field enhancement phenomena using ϵ -near-zero (ENZ) substrates for incident TM-polarized fields. When material losses are present a moderate field enhancement is achieved for a fairly wide frequency band and incident angles. In contrast, when material losses are partly compensated we observe much stronger field enhancement for narrower frequency band and incident angles. We show that the combination of low material losses, intended in the sense of small $\text{Im}(\epsilon)$, and ENZ condition may lead to even higher absorption. However, this feature may be used to trigger and enhance low-threshold nonlinear phenomena despite increased pump losses.

1. Introduction

Recently, artificial composite materials exhibiting ϵ -near-zero (ENZ) capabilities [1] have attracted a great deal of attention in view of potential applications, including tunnelling of electromagnetic energy [2], boosting of optical nonlinearities [3], low-threshold nonlinear effects [4-5], and producing narrow directive beams [6]. Here we clarify the conditions to maximize field enhancement. In particular, we analyze the setup reported in Fig. 1, where we consider an ENZ substrate with thickness h along the z direction. We consider natural ENZ materials, although artificial composites will be investigated and shown during the presentation. Representative examples of such artificial composite materials are made of N layers of plasmonic nanoparticles with inter-particle separation a (i.e., $h = Na$) as in [7-8].

2. Optical setup and formulation

We analyze TM-polarized plane wave incident obliquely on the sample shown in Fig. 1. The incident electric field lies on the x - z plane, i.e. $\mathbf{E}_1 = E_0 (\cos\theta_i \hat{\mathbf{x}} - \sin\theta_i \hat{\mathbf{z}}) e^{-j\mathbf{k}\cdot\mathbf{r}}$, where E_0 is the amplitude, θ_i the incident angle, $\mathbf{k} = k_x \hat{\mathbf{x}} + k_z \hat{\mathbf{z}} = k_1 (\sin\theta_i \hat{\mathbf{x}} + \cos\theta_i \hat{\mathbf{z}})$ the wavevector, $\mathbf{r} = x\hat{\mathbf{x}} + z\hat{\mathbf{z}}$, $k_{1,2} = k_0 \sqrt{\epsilon_{1,2}}$, k_0 the free space wavenumber, and $\epsilon_{1,2}$ the relative permittivities of the surrounding medium and substrate, respectively. From Snell's law we know that $\sqrt{\epsilon_1} \sin\theta_i = \sqrt{\epsilon_2} \sin\theta_t$, where θ_t is the angle of refraction inside the substrate (see Fig. 1). The electric field \mathbf{E}_2 inside the substrate is given by $\mathbf{E}_2 = AE_0 (\cos\theta_t \hat{\mathbf{x}} - \sin\theta_t \hat{\mathbf{z}}) e^{-jk_2(x\sin\theta_t + z\cos\theta_t)} + BE_0 (\cos\theta_t \hat{\mathbf{x}} + \sin\theta_t \hat{\mathbf{z}}) e^{-jk_2(x\sin\theta_t - z\cos\theta_t)}$, where A and B are the coefficients of forward and backward waves inside the substrate. Because of continuity of the displacement field at the boundary, $\epsilon_1 E_{z1} = \epsilon_2 E_{z2}$, the longitudinal component of the electric field

E_{z2} inside the substrate tends to become singular when $\epsilon_2 \sim 0$. This component is analyzed in the next section for varying frequency and incident angles. In the ideal, lossless case, two conditions are observed: (i) at the critical angle $\theta_i = \theta_i^C$, for which $k_{z2} = k_0 \sqrt{\epsilon_2 - \epsilon_1 \sin^2 \theta_i^C} = 0$, with $\epsilon_2 \neq 0$, E_{z2} takes on large, finite values for specific physical parameters; (ii) at a general $\theta_i \neq 0$, for $\epsilon_2 = 0$, total reflection takes place and $E_{z2} \rightarrow \infty$. When material losses are present, θ_i^C becomes complex, and the described properties, though less pronounced, can be used for enhancing absorption.

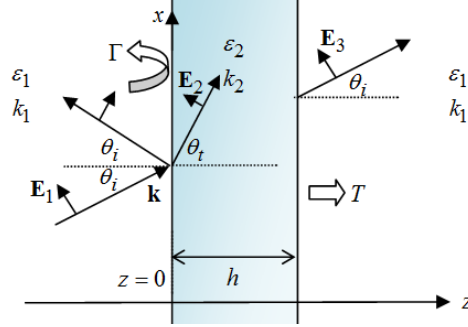


Fig. 1: ENZ setup under analysis, with $|\epsilon_2| \ll 1$. ENZ leads to high absorption.

3. Subwavelength ENZ substrate: linear and nonlinear properties

As an example, we consider a substrate of subwavelength thickness $h = 20$ nm made of CaF_2 , which naturally exhibits $\epsilon_{\text{CaF}_2} \approx 0 - j0.166$ at $21.08 \mu\text{m}$ [9] (therefore here $\epsilon_2 \equiv \epsilon_{\text{CaF}_2}$). The surrounding medium has $\epsilon_1 = 1$. The normalized field intensity $|E_{z2,n}|^2 = |E_{z2}|^2 / |E_0|^2$ computed at $z = h/2$ as a function of wavelength and incident angle inside the substrate is shown in Fig. 2(a). Then, assuming an artificial material loss compensation mechanism (that may involve the inclusion of gain material) for lowering $\text{Im}(\epsilon_{\text{CaF}_2})$ to for example a value of $\epsilon_{\text{CaF}_2}^{**} = \text{Re}(\epsilon_{\text{CaF}_2}) - j \text{Im}(\epsilon_{\text{CaF}_2}) / 10$, we calculate again $|E_{z2,n}|^2$ (Fig. 2(b)). Three properties are observed: (i) when natural material losses are considered, $|E_{z2,n}|^2$ approaches a maximum factor 30 for a wide frequency/incident angle band and take on a characteristic tear-drop shape; (ii) the artificial compensation of $\text{Im}(\epsilon_{\text{CaF}_2})$ allows $|E_{z2,n}|^2$ to peak at ~ 1700 , for a narrower frequency/incident angle band; (iii) the angle of maximum field enhancement shifts toward smaller incident angles as the imaginary part of the permittivity is reduced. These results suggest that the introduction of an artificial material loss compensation mechanism may boost local field intensities significantly, leading to enhanced nonlinear optical phenomena. In order to shed some light on the effects of material loss compensation on nonlinear properties of ENZ materials, we investigated third harmonic generation from a $h = 20$ nm thick slab of two different materials: (i) CaF_2 , with permittivity ϵ_{CaF_2} [9]; and (ii) CaF_2^{**} , with permittivity $\epsilon_{\text{CaF}_2}^{**}$. For both cases and all incident angles pump irradiance is 10 MW/cm^2 at $21.08 \mu\text{m}$, where $\epsilon_{\text{CaF}_2} \approx 0 - j0.166$. We assumed a non-dispersive, nonlinear susceptibility of bulk CaF_2 equal to $\chi^{(3)} = 10^{-21} \text{ m}^2/\text{V}^2$ [10]. We evaluate the total third harmonic conversion efficiency as $\eta_{\text{TH}} = P_{3\omega} / P_\omega$, where $P_{3\omega}$ and P_ω are the radiated power at the third harmonic and the input pump power, respectively [11]. Fig 2(c) shows η_{TH} at $21.08 \mu\text{m}$ as a function of the incident pump angle. The maximum efficiency for natural CaF_2 occurs at $\sim 88^\circ$ (blue curve), while the maximum efficiency angle for CaF_2^{**} is $\sim 70^\circ$ (black, dashed line). In both cases examined, with natural material losses and with material loss compensation, the nonlinear behavior tracks rather well the field intensity enhancement (compare the blue line in Fig. 2(c) with Fig 2(a), and black line in with Fig. 2(b), both obtained from a cut at $21.08 \mu\text{m}$). We note from Fig. 2(b) that the local absorption rate,

defined as $A = \text{Im}(\epsilon_0 \epsilon_2) |E_2|^2$, with $|E_2|^2 = |E_{x2}|^2 + |E_{z2}|^2$, actually increases with respect to the case discussed in Fig. 2(a), despite the decrease in $\text{Im}(\epsilon_2)$ due to the huge local field enhancement. At the same time the maximum efficiency angle decreases, following a behavior similar to the field intensity enhancement (Fig. 2(b)). One should also notice that the engineered CaF_2^{**} that includes gain shows a dramatic increase of conversion efficiency (~ 7 orders of magnitude) that cannot be predicted solely by the observation of local field enhancement.

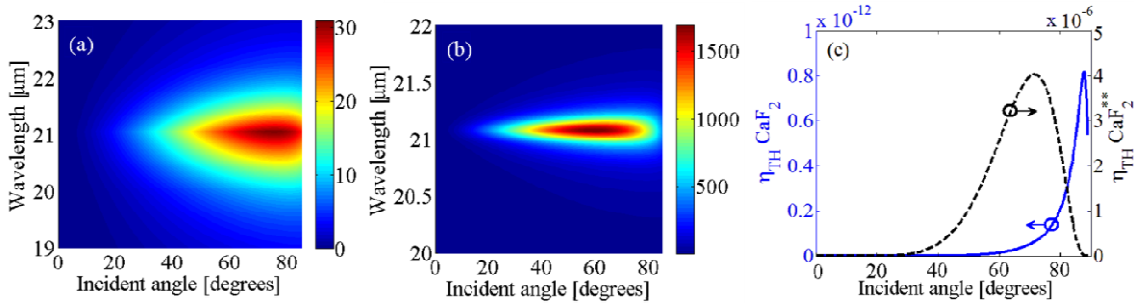


Fig. 2: Normalized field intensity $|E_{z,2,n}|^2$ at $z = h/2$ versus wavelength and incident angle, for (a) ϵ_{CaF_2} and (b) $\epsilon_{\text{CaF}_2}^{**}$. (c) Third harmonic conversion efficiency versus pump incident angle for CaF_2 (solid blue line) and CaF_2^{**} (dashed black line). Note the 8 orders of magnitude difference of the left and right efficiency scales.

4. Conclusion

We have analyzed local field enhancement in ENZ substrates illuminated by incident TM-polarized fields. We find that strong enhancement may be achieved for a limited frequency band when the material has very small losses and for a given incidence angle. Therefore, if material losses are compensated ($\text{Im}(\epsilon) \sim 0$) at the ENZ condition, the boost in the field enhancements may then be effectively exploited to significantly lower the threshold of nonlinear processes, such as optical switching and bistability, despite increased pump absorption. As an example we showed that an artificial reduction of material losses by one order of magnitude leads to a 7 orders of magnitude increase in the third harmonic conversion efficiency from an extremely subwavelength ($\sim \lambda/1000$) slab of CaF_2 .

References

- [1] N. Garcia, E. V. Ponizovskaya, and J. Q. Xiao, Zero permittivity materials: Band gaps at the visible, *Applied Physics Letters*, vol. 80, pp. 1120-1122, 2002.
- [2] M. Silveirinha and N. Engheta, Tunneling of Electromagnetic Energy through Subwavelength Channels and Bends using ϵ -Near-Zero Materials, *Physical Review Letters*, vol. 97, p. 157403, 2006.
- [3] C. Argyropoulos, P.-Y. Chen, G. D'Aguanno, N. Engheta, and A. Alù, Boosting optical nonlinearities in ϵ -near-zero plasmonic channels, *Physical Review B*, vol. 85, p. 045129, 2012.
- [4] A. Ciattoni, C. Rizza, and E. Palange, Extreme nonlinear electrodynamics in metamaterials with very small linear dielectric permittivity, *Physical Review A*, vol. 81, p. 043839, 2010.
- [5] M. A. Vincenti, D. de Ceglia, A. Ciattoni, and M. Scalora, Singularity-driven second- and third-harmonic generation at ϵ -near-zero crossing points, *Physical Review A*, vol. 84, p. 063826, 2011.
- [6] G. Lovat, P. Burghignoli, F. Capolino, D. R. Jackson, and D. R. Wilton, Analysis of directive radiation from a line source in a metamaterial slab with low permittivity, *IEEE Transactions on Antennas and Propagation*, vol. 54, pp. 1017-1030, Mar 2006.
- [7] S. Campione, M. Albani, and F. Capolino, Complex modes and near-zero permittivity in 3D arrays of plasmonic nanoshells: loss compensation using gain [Invited], *Optical Materials Express*, vol. 1, pp. 1077-1089, 2011.
- [8] S. Campione, S. Steshenko, M. Albani, and F. Capolino, Complex modes and effective refractive index in 3D periodic arrays of plasmonic nanospheres, *Optics Express*, vol. 19, pp. 26027-26043, 2011.
- [9] E. Palik, *Handbook of Optical Constants of Solids*. New York: Academic Press, 1985.
- [10] V. Gordienko, N. Khodakovskij, P. Mikheev, F. Potemkin, and K. Zubov, THG in dielectrics using low-energy tightly-focused femtosecond laser: third-order nonlinearity measurements and the evolution of laser-induced plasma, *Journal of Russian Laser Research*, vol. 30, pp. 599-608, 2009.
- [11] R. W. Boyd, *Nonlinear Optics*, New York: Academic Press, 2003.